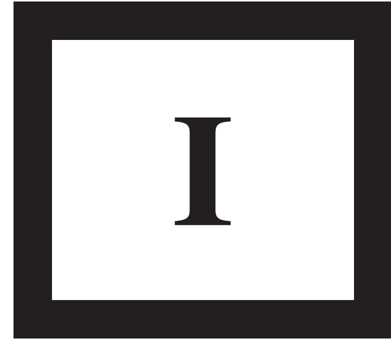

Publication I

F. Boxberg and J. Tulkki, *Modeling of oxidation-induced strain and its effect on the electronic properties of Si waveguides*, IEEE Transactions On Electron Devices **48**, pp. 2405-2409 (2001).

© 2001 IEEE

Reprinted with permission.

This material is posted here with permission of the IEEE. Such permission of the IEEE does not in any way imply IEEE endorsement of any of Helsinki University of Technology's products or services. Internal or personal use of this material is permitted. However, permission to reprint/republish this material for advertising or promotional purposes or for creating new collective works for resale or redistribution must be obtained from the IEEE by writing to pubs-permissions@ieee.org.

By choosing to view this document, you agree to all provisions of the copyright laws protecting it.

©2001 IEEE. Reprinted, with permission, from F. Boxberg and J. Tulkki, IEEE Transactions on Electron Devices Vol. 48, Issue 10, Pages 2405-2409 (2001)

Modeling of Oxidation-Induced Strain and Its Effect on the Electronic Properties of Si Waveguides

Fredrik Boxberg and Jukka Tulkki

***Abstract*—We have studied the influence of oxidation-induced strain on the electronic structure in Si quantum wires and quantum point contacts. The strain calculations were done using a semiempirical approximation which enabled three-dimensional (3-D) strain simulations of the device structures. The strain-induced deformation of the conduction band gives rise to a 3-D potential minimum having a depth of ∼35 meV. In addition to the formation of localized electron states in the channel, our calculations predict crossing of transverse energy levels corresponding to different conduction band minima. Our calculations also predict strain-induced channeling of electrons to the edges of the structure.**

***Index Terms*—Quantum point contact, quantum wire and strain, silicon, thermal oxidation.**

I. INTRODUCTION

THE OXIDATION-induced strain is one of the possible origins of the observed complicated conductance characteristics in Si/SiO_2 electron waveguides [1], [2]. We have studied the influence of strain on the electronic structure in Si quantum wires (QWR) and quantum point contacts (QPC) fabricated on (001) silicon on insulator (SOI) wafers. Our work is motivated by a recent study of these device structures by Gustafsson *et al.* [3], [4]. The strain field in these structures is three-dimensional (3-D), making numerical solution of the visco-elastic continuum model very difficult. In this work, we analyze the strain field using a semi-empirical method, which we have compared with analytic models for 3-D structures of higher symmetry. The structures of Gustafsson *et al.* were fabricated by using electron-beam lithography and etching followed by narrowing of the conducting channel by thermal oxidation. Fig. 1 shows a fabricated Si QWR structure [3]. The active channel is in the middle of Fig. 1. The direction of the current is vertical, which corresponds to the $\langle 110 \rangle$ crystal direction.

These waveguide structures are of potential interest since their fabrication includes processing steps similar to those used in the CMOS process. In addition, the binding energies of electrons are high since confinement is governed by the band-edge difference between the surrounding SiO_2 and the conducting Si channel. This may allow high temperature operation in the future. However, all lithographically defined Si waveguides have, so far, shown complicated resonance structures in the current–voltage (I–V) characteristics [1], [2]. These have been addressed to the increased scattering from the large interface area and the possible oxidation-induced strain in the structure. The Si/SiO_2 interface region contains oxide charges that reduce the conductivity of the Si. In very narrow Si channels, the oxide charges could prevent ballistic transport of the electrons because of the increased scattering. The role of oxidation-induced strain on the electronic properties of Si wave guides has remained largely unexplored and will be discussed in this work.

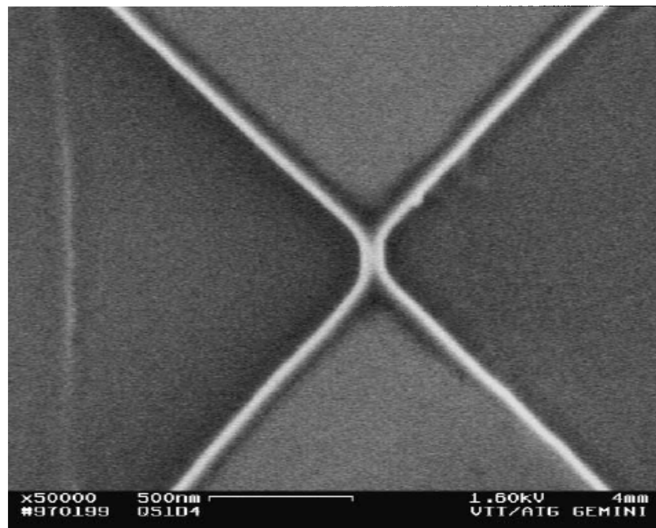

Fig. 1. Scanning electron micrograph of a fabricated QWR covered by the gate oxide on a SOI wafer. The gate metal has been removed [4].

The strain in Si/SiO_2 structures is mainly created during the oxidation of gate oxides or isolation trenches. The thermal oxidation process and the creation of oxidation-induced strain was modeled successfully by Kao *et al.* [5], [6] for the axially symmetric case. In this model, the oxide is thought of as a Newtonian fluid, i.e., an incompressible, viscous fluid. In reality, the oxide is visco-elastic, which means that the properties of the material are between solid and liquid. Different visco-elastic models including, e.g., the Kelvin–Voigt and the Maxwell model have been discussed in [7]. If the visco-elastic properties of SiO_2 were known as a function of temperature and strain, it would in principle be possible to make a realistic simulation of the oxidation process by using an iterative scheme in which the visco-elastic properties could be updated at each differential oxidation step [7].

A limitation of the continuous medium calculations is that they are based on the Deal–Groove approximation for oxidation (DG model) [8]. Within the DG model, the gradient of the

Manuscript received December 6, 2000; revised July 6, 2001. This work was supported by the Academy of Finland under Contract 46807. The review of this paper was arranged by Editor J. Hollenhorst.

The authors are with the Laboratory of Computational Engineering, Helsinki University of Technology (HUT), Fin-02015 HUT, Espoo, Finland (e-mail: fredrik.boxberg@hut.fi; jukka.tulkki@hut.fi).

Publisher Item Identifier S 0018-9383(01)08359-9.

0018–9383/01$10.00 © 2001 IEEE

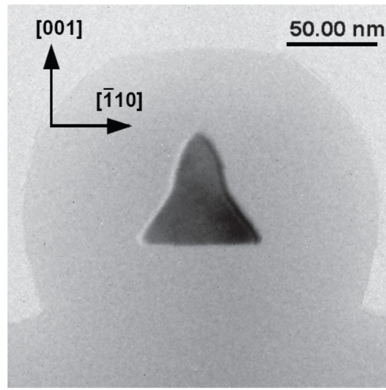

Fig. 2. This figure corresponds to the same original TEM picture as [3, Fig. 2(b)] (J. Ahopelto, private communications). Note that this figure represents a cross section of regular Si/SiO_2 wires, which before the oxidation have dimensions similar to the narrowest constriction of the present QPC structure (before oxidation). The dark grey region is the Si core inside the thermal SiO_2.

oxidant species is assumed constant over the oxide film, and the chemical reaction between Si and O_2 is assumed to take place at a sharp Si/SiO_2 interface. In [9], de Almeida has proposed an improved model for the diffusion–chemical reaction process. However, detailed description of the growth of thin oxide films is possible only by molecular dynamics methods.

High resolution measurement of strain in ultrasmall structures is difficult. In most cases, the comparisons are made between calculated and measured oxide thicknesses. However, there are few experiments in which the oxidation induced strain has been monitored. EerNisse [10] studied the strain in the oxidation of planar Si structures and found that dry oxidation in temperatures above 950 °C induces no in-plane stresses. In the experiment by Kim *et al.* [11], dry oxidation in 780 °C was found to create in-plane stresses of 0.96%.

II. Geometrical Model of the QWR

The geometrical model used in our strain calculation is based on TEM images of the fabricated structure. Fig. 2 is a TEM image of a quantum wire (QWR) in the $\langle 110 \rangle$ direction [3]. The starting point of the thermal oxidation was a rectangular Si wire on top of a buried-oxide layer. The faster oxidation rate at the (111) facets has created an almost triangular cross-section. The rounded corners and the deviation from ideal crystal planes are the results of a slower oxidation rate caused by the larger strain. It is also evident that there has been diffusion of oxygen through the buried oxide and therefore, the wire has been oxidized from below even if the oxidation rate is slower at the bottom of the wire. TEM images [3] show that the oxidation from below can take place also in the leads where the distance from SiO_2/air interface is several hundreds of nanometers [3].

The computational model of a QWR is shown in Fig. 3. The conducting Si (light gray) is completely surrounded by the boundary layer (black). This structure is then embedded in thermal SiO_2 created in the gate oxidation. Below the thermal SiO_2, there is the buried SiO_2 of the SOI wafer. The length of the conductive channel connecting the leads, was varied between 120 nm and 240 nm. The shape and the dimensions of the channel in our model was the same as in Fig. 2.

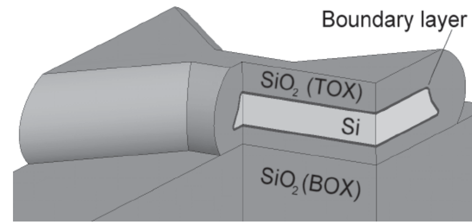

Fig. 3. Structural model for a QPC. The light and darker gray indicate the Si and the thermal SiO_2, respectively. The black region is the 4-nm thick boundary layer.

III. Semi-Empirical Model for the Oxidation-Induced Strains

The oxidation-induced strain was calculated by a semi-empirical method, in which the strain is caused by elastic expansion of a boundary oxide layer close to Si/SiO_2 interface. The model was developed first for a cylinder structure having the same oxide and Si radii as the narrowest constriction in the present 3-D devices. Test calculations showed that when a 4-nm thick boundary layer was let to expand by an appropriate factor the strain in the silicon channel and the oxide become very close to the strain predicted by the hydrodynamical oxidation model of Kao [6]. In the analytic model of Kao, the radial stress in the oxide is given by

$$\sigma_{rr} = 2\eta\xi \left(\frac{1}{b^2} - \frac{1}{r^2} \right) \tag{1}$$

and the hoop stress by

$$\sigma_{\theta} = 2\eta\xi \left(\frac{1}{b^2} + \frac{1}{r^2} \right) \tag{2}$$

where η is oxide viscosity, and ξ is a constant describing oxidation velocity. In the analytic model, these parameters are considered independent of stress. In (1) and (2), r is the distance from the axis of the cylinder and b is the radius of the Si/SiO_2 interface. When normalized on the axis of the channel our model has a relative error less than 6% except for the boundary layer in which the error is substantially larger. However, this will not influence the electronic structure calculations much because of the large band gap difference between Si and SiO_2, i.e., the wave functions do not penetrate to this region. A further source of error is the neglectance of the strain-relaxation during the down-cooling from 1000 °C to room temperature due to differences in the coefficients of thermal expansion coefficients. This error is estimated to be $\sim 0.25\%$. This effect was neglected in our simulations since the oxidation-induced strain was of the order of 1%. The benefit of our approach is that strain calculations become feasible even for complicated 3-D device structures. We can also account for the anisotropic oxidation effects semi-empirically, since the geometry of our models is taken from TEM studies of the fabricated devices.

In our 3-D simulations we have used the hydro-dynamical model as our reference data. From this model we have estimated that the strain in a solid Si/SiO_2 cylinder can exceed 1%, when the dimensions are of the same order as the diameter of our Si channel. The expansion of the boundary layer, in our 3-D simulations, was normalized so that, in the case of an ideal cylin-

TABLE I
STRUCTURAL PARAMETERS USED IN THE FEM CALCULATIONS

Material	E	ν_{xy}	Ref
Si	168.9 GPa	0.262	[13]
SiO_2	71.4 GPa	0.16	[13]

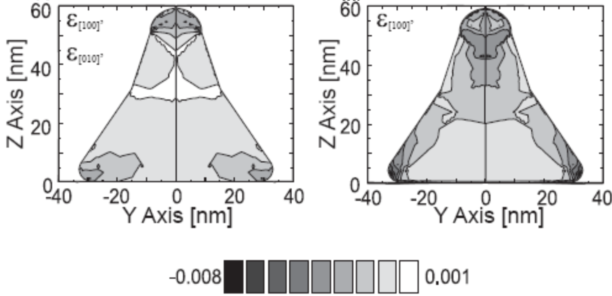

Fig. 4. Diagonal strain components in a transverse plain located in the middle of the construction.

drical geometry the radial strain was 1%. The magnitude of the 3-D strain distribution scales almost linearly of the expansion coefficient of the boundary layer. Hence, the qualitative result of the simulations is assumed to depend very little on the normalization.

IV. STRAIN CALCULATIONS

The elastic expansion of the boundary layer takes place in a direction perpendicular to the Si/SiO_2 interface. This was achieved by the use of several local coordinate systems. For more complex interfaces like saddle surface we need to approximate the situation. The strain induced by this expansion was calculated by finite element method (FEM) [12]. Table I gives the material parameters used in the calculations. In FEM, we used a tetrahedric structural solid element in all simulations. The quadratic element has ten nodes, of which each node has three translational degrees of freedom. Because of practical reasons, the number of nodes in the element meshing was limited to 10^5.

When calculating the strain, the largest errors are created at the abrupt Si/SiO_2 interface, but these problems are also expected in other numerical evaluations of the stresses. By making the calculation meshing dense enough, this error can be made sufficiently small.

Fig. 4 shows the linear strain components in the middle of the channel. The oxide is left out from this contour plot for clarity. The ε_{100} and the ε_{010} components will be equal because of the symmetries at this (110) plane. The largest strains are found in the corners of the triangular wire. and ε_{001} is the largest of the three strain components. Further away from the channel and from the Si/SiO_2 edges, the strain approaches zero asymptotically.

V. POTENTIAL MINIMA IN THE CONDUCTION BAND AND VALLEY SPLITTING

The simulated strain was converted into deformation of the six energy valleys by the $\mathbf{k} \cdot \mathbf{p}$ theory [14]. The strain is incor-

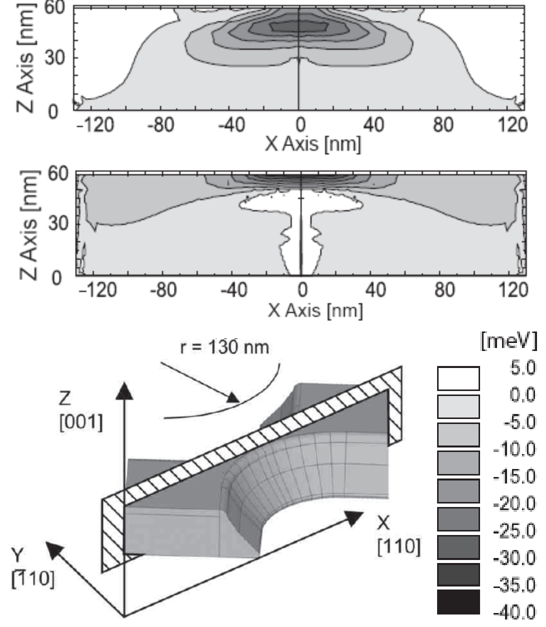

Fig. 5. Strain-induced deformation of the three energy valley pairs in the middle of the Si channel. The first contour plot corresponds to the $[\pm a,\ 0,\ 0]$ and the $[0,\ \pm a,\ 0]$ valleys, while the second corresponds to the $[0,\ 0,\ \pm a]$ valleys. The lower image shows how the contour plots are taken.

porated into the band structure as a perturbation term given by

$$H_\varepsilon = \sum_{\alpha,\,\beta=1}^{3} D^{\alpha\beta} \varepsilon_{\alpha\beta} \tag{3}$$

where $\varepsilon_{\alpha\beta}$ are the strain tensor elements, and $D^{\alpha\beta}$ are the deformation potential constants [15]. By accounting for the symmetry of the diamond lattice the diagonal terms of the Hamiltonian (3) for the $\langle 100 \rangle$ minima are given by

$$\delta E^{(100)} = D^{[100]} \varepsilon_{[100]} + D^{[010]} \left(\varepsilon_{[010]} + \varepsilon_{[001]} \right). \tag{4}$$

Using conventional notations $D^{[100]} = \Xi_d^{(100)} + \Xi_u^{(100)}$ and $D^{[010]} = \Xi_d^{(100)}$, we obtain [14]

$$\delta E^{(100)} = \Xi_d^{(100)} \left(\varepsilon_{[100]} + \varepsilon_{[010]} + \varepsilon_{[001]} \right) + \Xi_u^{(100)} \varepsilon_{[100]}. \tag{5}$$

For the other minima, we have by symmetry

$$\delta E^{(010)} = \Xi_d^{(100)} \left(\varepsilon_{[100]} + \varepsilon_{[010]} + \varepsilon_{[001]} \right) + \Xi_u^{(100)} \varepsilon_{[010]} \tag{6}$$

$$\delta E^{(001)} = \Xi_d^{(100)} \left(\varepsilon_{[100]} + \varepsilon_{[010]} + \varepsilon_{[001]} \right) + \Xi_u^{(100)} \varepsilon_{[001]}. \tag{7}$$

The anisotropy term in (5)–(7) gives rise to a lowering of the degeneracy in strained Si. In Fig. 5, we have plotted the deformation potential energy for the energy valleys at a cross section taken along the channel. In the middle of the channel, there is a ~ -35 meV deep minimum for the $[0,\ 0,\ \pm a]$ valleys. Also, the other four valleys show a clear minimum in the middle of the channel. However, the geometrical size of these minima is smaller and they are more shallow.

The deformation will lead to a lowering of the conduction band degeneracy. The $[0,\ 0,\ \pm a]$ minima are slightly below the $[\pm a,\ 0,\ 0]$ and $[0,\ \pm a,\ 0]$ valleys in the leads, which are outside the area shown in Fig. 6. This splitting into two- and four-fold

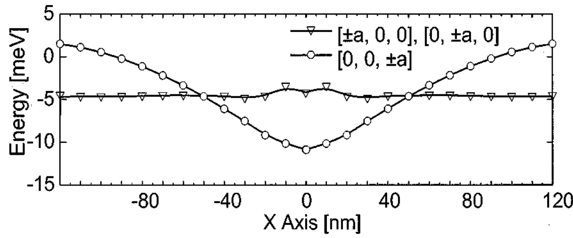

Fig. 6. Splitting of the subbands is plotted as function of the x-axis. The deformation potential energy is averaged over the z coordinate. The strain induces a band splitting of about 7 meV.

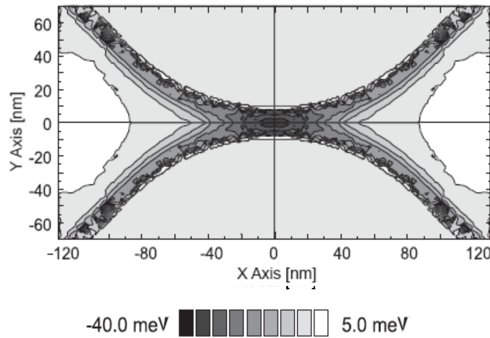

Fig. 7. Deformation potential energy for the $[0,\ 0,\ \pm a]$ valleys at $z = 50$ nm. The white color near the Si/SiO_2 interface corresponds to $+20 - +30$ meV.

degeneracies (spin-degeneracy not included) is enhanced by the deformation potential. The effect is visualized in Fig. 6, where we have plotted the position of the energy valleys along the center line of the channel. The value of the deformation potential energy is averaged over the z coordinate.

Another interesting result is the formation of channels along the edges of the Si structure. The strain is proportional to the curvature of the Si/SiO_2 interface and therefore, the curved edges of the Si QPC will be strain sources. It is difficult to predict how much the induced minima along the edges will affect the conductance of the device. However, the strain-induced minima will bring the conductance electrons closer to the Si/SiO_2 interface in the leads and thereby enhance the interface and ionic charge scattering. Fig. 7 shows the deformation potential energy for the $[0,\ 0,\ \pm a]$ valleys at $z = 50$ nm. In this figure, the white color near the Si/SiO_2 interface corresponds to $\sim +20 - +30$ meV.

The strain-induced deformation potential minima can confine several electrons for a long Si channel. This was verified by finite difference calculations where we solved one band eigenfunctions for one electron in the $[0,\ 0,\ \pm a]$ valleys. The strain is expected to be larger in thinner wires and therefore, bound electronic states are likely to exist also in narrow structures.

We calculated the confinement energies of few lowest transverse states for a 120-nm long QWR. The eigenstates solved for transverse states in the middle of the QWR. The eigenenergies for the lowest states of [001] minima were -25.3 meV, -20.2 meV, -16.5 meV, and -16.0 meV. These energies do not include the longitudinal quantization energy, which is smaller than 1 meV for all these states. Our results for the QWR are very close to the asymptotical limit of infinitely long wires because of the small longitudinal quantization energy. The ground state confinement energy obtained in the present calculation is 5 meV smaller than that obtained in our previous work [16], which was, however, based on a much simpler strain model. A prominent channeling effect can be seen in the wave functions. In the present calculation, the strain and the deformation potential take their largest value in the corners of the wire where the curvature of the Si/SiO_2 interface is largest. Therefore, electrons are confined to the top corner of the wire (three lowest states) or to the side corners (fourth eigenstate) (see Fig. 8). This will enhance the interface scattering. For the [100] and [010] minima, the lowest confinement energies are -7.7, -5.9, -4.2, and -2.5 meV, respectively. For these minima, the longitudial quantization gives significant contribution making the confinement effect fairly small.

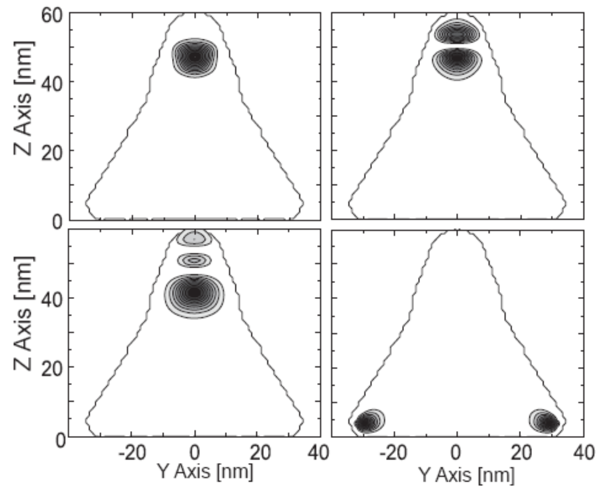

Fig. 8. Electron density of the ground state and three excited states in a qwr. The ground state energy was -25.3 meV.

VI. Potential Minima in the Conduction Band and Valley Splitting

In conclusion, we have shown that the oxidation-induced strain can markedly influence the electronic structure in Si/SiO_2 electron wave guides. We have made 3-D simulations of the strain in Si QWRs and QPCs fabricated on SOI wafers. Our approach is semi-empirical in the sense that we need experimental reference data for a simple 3-D model as a starting point to the calculation. Even though our assumptions of the magnitude of the strain are not exact for all oxidation conditions, we expect that the model gives good qualitative picture of the strain distribution. We have shown that the oxidation induces a -35 meV deep potential minimum in the narrowest constriction of the devices for the $[0,\ 0,\ \pm a]$ valleys of the conduction band. Potential minima are induced along the edges of the Si constriction, which could give rise to channeling effect and thereby increase interface and static charge scattering. The anisotropic coupling from the strain to the conduction band will also induce a level crossing for transverse states belonging to different conduction band valleys in the channel. We conclude that the oxidation-induced strain is a possible origin to the observed complicated conductance characteristics in Si/SiO_2 electron waveguides. We note that the present semiempiricial approach is no substitute to strain and temperature dependent visco-elastic continuum model, which enables calculation of strain distribution from the know values of material constants.

ACKNOWLEDGMENT

The authors would like to thank R. Lindgren for his help with the FEM calculations, and J. Ahopelto and M. Prunnila for fruitful discussions and interesting comments.

REFERENCES

[1] H. Namatsu, S. Horiguchi, M. Nagase, and K. Kurihara, "Fabrication of one-dimensional nanowire structures utilizing crystallographic orientation in silicon and their conductance characteristics," *J. Vac. Sci. Technol. B.*, vol. 15, no. 5, pp. 1688–1696, 1997.

[2] H. Ishikuro and T. Hiramoto, "On the origin of tunneling barriers in silicon single electron and single hole transistors," *J. Appl. Phys. Lett.*, vol. 74, pp. 1126–1128, 1999.

[3] A. Gustafsson, J. Ahopelto, M. Kamp, M. Emmerling, and A. Forchel, "Transmission electron microscopy studies of silicon-based electron waveguides fabricated by oxidation of etched ridges on buried oxide layers," in *Proc. Microscopic Semiconductor Materials Conf.*, Oxford, U.K., 1999, pp. 455–458.

[4] J. Ahopelto, M. Prunnila, M. Kamp, M. Emmerling, A. Forchel, B. S. Sorensen, A. Kristensen, P. E. Lindelof, and A. Gustafsson, "Coulomb blockade and conductance quantization in narrow silicon channels," in *2000 Silicon Nanoelectronics Workshop, Workshop Abstracts*, Honolulu, HI, June 11–12, 2000, pp. 79–80.

[5] D.-B. Kao, J. P. McVittie, W. D. Nix, and K. C. Saraswat, "Two-dimensional thermal oxidation of silicon—I. Experiments," *IEEE Trans. Electron Devices*, vol. ED-34, pp. 1008–1017, 1987.

[6] ——, "Two-dimensional thermal oxidation of silicon—II. Modeling stress effects in wet oxides," *IEEE Trans. Electron Devices*, vol. 35, pp. 25–37, Jan. 1988.

[7] V. Senez, D. Collard, B. Baccus, M. Brault, and J. Lebailly, "Analysis and application of a visco-elastic model for silicon oxidation," *J. Appl. Phys.*, vol. 76, pp. 3285–3296, 1994.

[8] B. E. Deal and A. S. Groove, "General relationship for the thermal oxidation of silicon," *J. Appl. Phys.*, vol. 36, pp. 3770–3778, 1965.

[9] R. M. C. de Almeida, S. Goncalves, I. J. R. Baumvol, and F. C. Stedile, "Dynamics of thermal growth of silicon oxide films on Si," *Phys. Rev. B*, vol. 61, pp. 12 992–12 999, 2000.

[10] E. P. EerNisse, "Stress in thermal SiO_2 during growth," *J. Appl. Phys. Lett.*, vol. 35, pp. 8–10, 1979.

[11] Y. Kim and S. Choi, "Direct observation of Si lattice strain and its distribution in the Si(001)–SiO_2 interface transition layer," *J. Appl. Phys. Lett.*, vol. 71, pp. 3504–3506, 1997.

[12] "Swanson analysis systems," Ansys 5.5, Inc., Houston, PA, 1998.

[13] Y.-L. Shen, S. Suresh, and A. Blech, "Stresses, curvatures and shape changes arising from patterned lines on silicon wafers," *J. Appl. Phys.*, vol. 80, pp. 1388–1398, 1996.

[14] J. M. Hinckley and J. Singh, "Influence of substrate composition and crystallographic orientation on the band structure of pseudomorphic Si–Ge alloy films," *Phys. Rev. B*, vol. 42, pp. 3546–3566, 1990.

[15] C. G. Van de Walle and R. M. Martin, "Theoretical calculations of heterojunction discontinues in the Si/Ge system," *Phys. Rev. B*, vol. 34, pp. 5621–5633, 1986.

[16] F. Boxberg, R. Virkkala, and J. Tulkki, "Strain distribution and carrier confinement in Si/SiO_2 quantum point contacts and wires," *J. Appl. Phys.*, vol. 88, pp. 600–602, 2000.

Fredrik Boxberg received the M.S. degree in electrical engineering from the Helsinki University of Technology (HUT), Espoo, Finland, in 2000.

He joined the Laboratory of Computational Engineering, HUT, in 1998. He has been studying mesoscopic electronic devices of Si and compound semiconductors. He has mainly focused on numerical analyses and theoretical studies.

Jukka Tulkki received the M.S. and Ph.D. degrees from the Helsinki University Technology (HUT), Espoo, Finland, in 1980 and 1986, respectively.

He was a Research Associate and Senior Researcher with HUT and with the University of Helsinki, Helsinki, Finland, from 1986 to 1998. Since 1998, he has been Professor of computational engineering with HUT. His scientific interests are in the physics of semiconductor quantum structures, photoelectron and Auger electron spectroscopies, and X-ray scattering processes.